Nonlin. Processes Geophys. Discuss., https://doi.org/10.5194/npg-2017-53
Manuscript under review for journal Nonlin. Processes Geophys.
Discussion started: 18 October 2017

Nonlinear Processes in Geophysics
Discussions
Open Access
EGU

Experimental study of forced convection heat transport in porous media

Nicola Pastore[(1)], Claudia Cherubini[(2)], Dimitra Rapti[(3)], Concetta I. Giasi[(1)]

[1]DICATECh, Department of Civil, Environmental, Building Engineering, and Chemistry, Politecnico di Bari, Bari, Italy.

[2]Department of Physics & Earth Sciences, University of Ferrara, via Saragat 1 - 44122 Ferrara, Italy.

[3]New Energies And environment Company (NEA) via Saragat, 1 - 44122 Ferrara, Italy.

Correspondence to: Nicola Pastore (nicola.pastore@poliba.it) and Claudia Cherubini (chrcld@unif.it)

Abstract

The knowledge of the dynamics of forced convection heat transfer in porous media is relevant in order to optimize the efficiency of geothermal installations in aquifers.

In some applications groundwater is used directly as thermal fluid. The system uses one or several drilling holes to pump and deliver groundwater with a heat exchange system at surface (open loop). Other applications use vertical borehole heat exchangers without injection or extraction of groundwater (closed loop). In both systems the convection flow dynamics in porous media play an important role on the heat production.

The present study is aimed at extending this thematic issue through heat transport experiments and their interpretation at laboratory scale. An experimental study to evaluate the dynamics of forced convection heat transfer in a thermally isolated column filled with porous medium has been carried out. The behavior of two porous media having different grain sizes and specific surfaces has been observed. The experimental data have been compared with an analytical solution for one dimensional heat transport for local non thermal equilibrium condition. The interpretation of the experimental data shows that, the heterogeneity of the porous medium affects heat transport dynamics causing a channeling effect which has consequences on thermal dispersion phenomena and heat transfer between fluid and solid phases limiting the capacity to store or dissipate heat in the porous medium.

Nonlin. Processes Geophys. Discuss., https://doi.org/10.5194/npg-2017-53
Manuscript under review for journal Nonlin. Processes Geophys.
Discussion started: 18 October 2017

Introduction

The European Climate and Energy Framework for 2050 aims to shift from the massive use of fossil sources to others characterized by very low emissions. Among the renewables sources, geothermal energy is the only one which is available basically everywhere and at any time.

For this reason, in the recent years the use of groundwater as low-enthalpy geothermal resource for heating and cooling of buildings and for agricultural and industrial processes is growing.

One of the main limits for the development of low – enthalpy geothermal systems concerns the high cost of investment. Installation of geothermal energy systems requires high upfront capital investments that often exceed the expectations of depreciation expense, so the investment is therefore inconvenient and the economic benefits can only occur after a long time. It is therefore of extreme importance to further the understanding of the behaviour of hydrological systems as concerns heat transport. Studying heat transfer phenomena takes the advantage of the fact that the governing partial differential equations used to describe flow and transport processes in porous media are based on the same form of mass and/or energy conservation laws.

Several studies have been already carried out in this context with the aim of enhancing heat transfer phenomena in porous media for engineering processes. Theoretical and numerical research on convection heat transfer in porous media has used two different models for the energy equation: the local thermal equilibrium model and the local thermal non-equilibrium model.

Most of the studies have been focussed on investigating on the validity of the local thermal equilibrium assumption (LTE) between the solid and fluid phase, the influence of nonlinear flow patterns, and the existing relationship between thermal dispersion and flow velocity.

Koh and Colony (1974) carried out an analytical investigation of the performance of a heat exchanger containing a conductive porous medium using Darcy flow model, while Koh and Stevens (1975) performed an experimental study of the same problem. They have shown that for a constant heat flux boundary condition the wall temperature is significantly decreased by using a porous material in the channel.

Vafai and Tien (1981) have formulated a general mathematical model that takes into consideration the boundary and inertial (non Darcian) effects on flow and heat transfer in porous media. In analyzing these effects, they considered three flow resistances: the bulk damping resistance due to the porous structure, the viscous resistance due to the boundary, and the resistance due to the inertial forces.

Later, Vafai and Tien (1982) performed a numerical and experimental investigation of the effects of the presence of a solid boundary and inertial forces on mass transfer in porous media.

Kaviany (1985) studied laminar flow through a porous channel bounded by two parallel plates maintained at a constant and equal temperature by applying a modified Darcy model for transport of momentum.

Vafai and Kim (1989) considered fully developed forced convection in a porous channel bounded by parallel plates by applying Brinkman-Forchheimer-extended Darcy model to obtain a closed-form analytical solution.

Lauriat and Vafai (1991) presented a comprehensive review on flow and heat transfer through porous media for two basic geometries: flow over a flat plate embedded in a porous medium and flow through a channel filled with a porous medium.

Hadim (1994) carried out a numerical study to analyze steady laminar forced convection in a 1) fully porous and 2) partially porous channel filled with a fluid-saturated porous medium and containing discrete heat sources on the bottom wall.

He modelled the flow in the porous medium using the Brinkman-Forchheimer extended Darcy model.

Kamiuto and Saitoh (1994) examined theoretically the effects of several system parameters on the heat transfer characteristics of fully developed forced convection flow in a cylindrical packed bed with constant wall temperatures. They developed a two-dimensional model incorporating the effects of non-Darcy, variable porosity and radial thermal dispersion.

Hwang et al. (1995) performed a study of non-Darcian forced convection in an asymmetric heating sintered porous channel to investigate the feasibility of using this channel as a heat sink. The study showed that the particle Reynolds number significantly affected the solid-to-fluid heat transfer coefficients.

A review of literature indicates that the local thermal equilibrium assumption (LTE) between the solid and fluid phase is used in the majority of heat transfer applications involving porous media Mikowycz et al., (1999) proposed a modified energy equation that can be solved for very early departures from LTE conditions. Their results confirmed that local thermal equilibrium in a fluidized bed depends on the size of the layer, mean pore size, interstitial heat transfer coefficient, and thermophysical properties. They concluded that for a porous medium subject to rapid transient heating, the existence of the local thermal equilibrium depends on the magnitude of a dimensionless quantity (which they called the Sparrow number) containing the contributions of the flow in porous media, interstitial heat transfer, and general thermal conduction.

An in-depth analysis of non-thermal equilibrium is provided by Amiri and Vafai (1994, 1998).

Amiri and Vafai (1994) carried out a steady-state analysis of incompressible flow through a bed of uniform solid sphere particles packed randomly. The investigation was aimed at exploring the

influence of a variety of phenomena such as the inertial effects, boundary effects, and the effect of the porosity variation model together with the thermal dispersion effect on the momentum and energy transport in a confined porous bed. They also proved the validity of LTE assumption and the two-dimensionality effects on transport processes in porous media.

In a subsequent study, Amiri and Vafai (1998) realised a rigorous and flexible model to explore the heat transfer aspects in a packed bed made of randomly oriented spherical particles. Along with the generalized momentum equation they used a two-energy equation model to describe the thermal response of a packed bed. They explored the temporal impact of the non Darcian terms and the thermal dispersion effects on energy transport. In addition, they investigated on the LTE condition and the one dimensional approach under transient condition by formulating dimensionless variables that will serve as instruments in depicting the pertinent characteristics of energy transport in a packed bed.

Khalil et al. (2000) performed a numerical investigation of forced convection heat transfer through a packed pipe heated at the surface under constant heat flux showing the effects of particle Reynolds number, pipe-to-particle diameter ratios and Prandtl number. They showed that the average Nusselt number increases with both particle Reynolds number and Prandtl number. They concluded that packing pipes with a porous medium can provide heat transfer enhancement for the same pumping power.

Wu and Hwang (1998) investigated experimentally and theoretically flow and heat transfer dynamics inside an artificial porous matrix by using a modified version of the local thermal nonequilibrium model (LTNE) which neglected the effects of thermal dispersion in both fluid and solid. The results showed a highly non-Fourier behaviour which combined rapid thermal breakthrough with extremely long-tailing, that was attributed to disequilibrium between the fluid and the porous matrix. However, the adopted model was unable to fully capture the thermal breakthrough observed in some experimental runs. They concluded that heat transfer coefficient increases with the decrease in porosity and the increase in the particle Reynolds number.

Emmanuel and Berkowitz (2007) were able to successfully fit the thermal breakthrough curves obtained by Wu and Hwang (1998) by applying the continuous time random walk (CTRW) which provided an alternative description of heat transport in porous media. They argued that larger scale spatial heterogeneities in porous media present obstacles to both the equilibrium and the LTNE models and that CTRW would be particularly applicable to the quantification of heat transfer in naturally heterogeneous geological systems, such as soils and geothermal reservoirs.

Geological media are typically characterized by heterogeneities on many scales, resulting in a wide range of fluid velocities, porosities, and effective thermal conductivities.

Despite the uncertainty and contradiction in defining the thermal dispersion, several studies addressed the effects of thermal dispersion in porous media and different approaches have been developed to describe it (Hsu and Cheng, 1990; Anderson, 2005; Molina-Giraldo et al., 2011).

Thermal dispersion is generally defined as a function of fluid velocity and grain size (Lu et al., 2009, Sauty et al., 1982, Nield and Bejan, 2006).

According to Sauty et al. (1982) and Molina-Giraldo et al. (2011), the thermal dispersion is a linear function of flow velocity and relates to the anisotropy of the velocity field whereas Rau et al. (2012) proposed a dispersion model as a function of the square of the thermal front velocity.

The literature also contains conflicting theories about the magnitude of thermal dispersivity. Smith and Chapman (1983) state that it has the same order of magnitude as solute dispersivities, while Ingebritsen and Sanford (1999) neglect it. According to Vandenbohede et al. (2009) thermal dispersivities are small in comparison to solute dispersivities and less scale-dependent.

Mori et al. (2005) showed experimentally that, for water fluxes ranging between 0.6×10^{-6} and 0.3×10^{-3} (m/s) thermal dispersion was nearly independent of water flow and its effects were insignificant.

According to Rau et al., (2012), the effect of thermal dispersion on heat transport is significant for high values of thermal Peclet number. Also Metzger et al. (2004) introduced a dispersion model based on the thermal Peclet number.

Koch et al. (1989) obtained an analytical expression for the dispersion tensor for a regular arrangement of cylinders or spheres. They found that for high values of Peclet numbers, the ratio of longitudinal total thermal diffusivity to the fluid thermal diffusivity was proportional to the square of the Peclet number while maintaining the transverse dispersion constant. The analytic finding was in good concordance with the experimental measurements of Gunn and Pryce (1969).

Eidsath et al. (1983) quantified the longitudinal thermal dispersion and stressed that the streamwise ratio of longitudinal total thermal diffusivity to the fluid thermal diffusivity was proportional to $Pe^{1.7}$.

Ait Saada et al. (2006) investigated the behaviour of microscopic inertia and thermal dispersion in a porous medium with a periodic structure by using a local approach at the pore scale to evaluate the velocity and temperature fields as well as their intrinsic velocity and temperature fluctuations in a typical unit cell of the porous medium under study. They concluded that non-linear effects characterizing microscopic inertia might be the definitive cause of thermal dispersion depending on the nature of the porous medium and in certain situations can exceed 50% toward the contribution of thermal dispersion. Particularly for a highly conducting fluid moving with high Peclet numbers,

164 microscopic inertial effects showed to take a great part in the heat transfer duty. They concluded
165 that a considerable interaction between the velocity and thermal fields exists.
166 This work is aimed at studying the dynamics of forced convection heat transport in porous media
167 allowing the understanding of how the grain size and the specific surface affect heat transport in
168 terms of macrodispersion phenomena, heat transfer between solid and fluid phases and heat storage
169 properties. In particular, the present study involves the experimental investigation of heat transport
170 through a thermally isolated column filled with porous medium. Several heat tracer tests have been
171 carried out using porous media with different grain sizes. The experimental observed breakthrough
172 curves have been compared with the one dimensional analytical solution for the forced convection
173 heat transport in local thermal non equilibrium condition. The results highlight the effects of grain
174 size and the specific surface on forced convection heat transport dynamics in porous media.

175 **Theoretical background**

176 In several studies examining the flow dynamics through porous media it is assumed that flow is
177 described by Darcy's law, which expresses a linear relationship between pressure gradient and flow
178 rate. Darcy's law has been demonstrated to be valid at low flow regimes (Re<1), whereas for
179 Re>>1 a nonlinear flow behavior is likely to occur. As velocity increases, the inertial effects start
180 dominating the flow field. In order to take these inertial effects into account, Forchheimer (1901)
181 introduced an inertial term representing the kinetic energy of the fluid to the Darcy equation. The
182 Forchheimer equation for one dimensional flow in terms of hydraulic head h (L) is given as follows:

183 $$-\frac{dh}{dx} = \frac{\mu}{\rho g k} q + \frac{\beta}{g} q^2 \quad (1)$$

184 Where x (L), k (L^2) is the permeability, μ ($ML^{-1}T^{-1}$) is the viscosity, ρ (ML^{-3}) is the density, q (LT^{-1})
185 is the darcy velocity and β (L^{-1}) is called the non –Darcy coefficient.

186 Ergun (1952) derived a model for high velocity pressure loss in a porous medium from the
187 Forchheimer equation by correlating the permeability and inertial resistance dimensionally to the
188 porosity and the equivalent sphere diameter of rough particles. The permeability and inertial
189 coefficient are interpreted in terms of spatial parameters as follows:

190 $$k = \frac{d_p{}^2 n^3}{A(1-n)^2} \quad (2)$$

Nonlin. Processes Geophys. Discuss., https://doi.org/10.5194/npg-2017-53
Manuscript under review for journal Nonlin. Processes Geophys.
Discussion started: 18 October 2017

$$\beta = \frac{B(1-n)}{d_p n^3} \tag{3}$$

Where d_p (L) is the average particle diameter, n (-) is the porosity and the coefficients A = 180 and B = 1.8 are empirical values and were derived by averaging the Navier – Stokes equations for a cubic representative unit volume.

The behavior of convective heat transport in porous media is strongly dependent on the fluid velocity and the kinetics of heat transfer process between fluid and solid phases.

Given a packed bed, within a thermally isolated column of length L (L) in which a fluid flows with a specific flow rate q (LT^{-1}) and then with an average fluid velocity q/n, the initial temperature in the column is T_0 (K) and a continuous flow injection transports heat energy along the column. For a small ratio of column diameter D (L) to the length L and large fluid velocity the radial heat transport dynamics can be neglected in comparison with the axial dynamics. Then the heat transport dynamics in the porous medium column can be represented by a one dimensional model.

If the solid and fluid phases are in contact for a sufficient period of time, there is the possibility to establish a local thermal equilibrium (LTE) condition. In such case, only one energy equation is sufficient for the description of the convective heat transport through the porous medium. Assuming that porosity, densities and heat capacities are constant in time the energy equation for the fluid and solid phases are combined into a single equation as:

$$(\rho c)_{sf} \frac{\partial T_f}{\partial t} = \frac{\partial}{\partial x} \cdot \left[-v \rho_f c_f T_f + k_{sf} \frac{\partial T_f}{\partial x} \right] \tag{4}$$

With:

$$(\rho c)_{sf} = (1-n)\rho_s c_s + n \rho_f c_f \tag{5}$$

$$k_{sf} = (1-n) k_s + n k_f \tag{6}$$

Where T_f (K) is the temperature of the fluid, ρ_f (ML^{-3}) is the density of the fluid, ρ_s (ML^{-3}) is the density of the solid, c_f (LT^2K^{-1}) is the thermal capacitance of the fluid, c_s (LT^2K^{-1}) is the thermal capacitance of the solid, k_f ($MLT^{-3}K^{-1}$) is the thermal conductivity of the fluid, k_s ($MLT^{-3}K^{-1}$) is the thermal conductivity of the solid, whereas $(\rho c)_{sf}$ and k_{sf} represent the equivalent heat capacity and

Nonlin. Processes Geophys. Discuss., https://doi.org/10.5194/npg-2017-53
Manuscript under review for journal Nonlin. Processes Geophys.
Discussion started: 18 October 2017

thermal conductivity of the porous domain respectively including porosity and thermal properties of solid and fluid.

If the interaction between solid and fluid phase is rapid the solid and fluid phase cannot exchange sufficient amount of energy to establish local thermal equilibrium. At a given location solid and fluid phases have different temperatures. In the local thermal non equilibrium (LTNE) condition each phase needs an energy equation for the description of heat transport. Assuming that porosity, densities and heat capacities are constant in time, the energy equations can be written for the fluid and solid phase:

$$n\rho_f c_f \frac{\partial T_f}{\partial t} = \frac{\partial}{\partial x}\cdot\left[-vn\rho_f c_f T_f + nk_f \frac{\partial T_f}{\partial x}\right] + q_{fs} \tag{7}$$

$$(1-n)\rho_s c_s \frac{\partial T_s}{\partial t} = \frac{\partial}{\partial x}\cdot\left[(1-n)k_s \frac{\partial T_s}{\partial x}\right] - q_{fs} \tag{8}$$

The interaction between the two phases is represented by the sink/source terms q_{fs} given by following equation:

$$q_{fs} = hs_f\left(T_s - T_f\right) \tag{9}$$

Where h ($MT^{-3}K^{-1}$) is the convective heat transfer coefficient and s_f (L^{-1}) is the specific surface area.

The convective heat transfer coefficient is related to the Nusselt number Nu that for the porous medium can be expressed as:

$$\mathrm{Nu} = \frac{q_{fs} d_p}{k_f\left(T_f - T_s\right)} = \frac{hd_p}{k_f} \tag{10}$$

The hydrodynamic mixing of the interstitial fluid at the pore scale gives rise to significant thermal dispersion phenomena. Generally, the hydrodynamic mixing is due to the presence of obstruction, flow restriction and turbulent flow. Therefore, the equivalent thermal conductivity in equation (1) and thermal conductivity in equation (4) is replaced with the effective thermal conductivity k_{eff} which is the sum of thermal conductivity and thermal dispersion conductivity. The effective thermal conductivity depends on various parameters such as mass flow rate, porosity, shape of pores, temperature gradient, and solid and fluid thermal properties (Kaviany, 1995). The following equation can be used to estimate k_{eff}.

$$\frac{k_{eff}}{k_f} = \frac{k}{k_f} + K \cdot \mathrm{Pe}^a \tag{11}$$

Pe represents the Peclet number defined as the product between the Reynolds number Re and Prandtl number Pr;

$$\mathrm{Pe} = \mathrm{Re} \times \mathrm{Pr} = \frac{\rho_f v d_p}{\mu} \times \frac{c_f \mu}{k_f} = \frac{v d_p}{D_f} \tag{12}$$

The energy equation representative of the local thermal non equilibrium can be written as:

$$\frac{\partial T_f}{\partial t} = -v\frac{\partial T_f}{\partial x} + D_{eff}\frac{\partial^2 T_f}{\partial x} + \alpha\left(T_s - T_f\right) \tag{13}$$

$$\frac{1-n}{n}\frac{\rho_s c_s}{\rho_f c_f}\frac{\partial T_s}{\partial t} = \frac{1-n}{n}\frac{k_s}{\rho_f c_f}\frac{\partial^2 T_s}{\partial x} - \alpha\left(T_s - T_f\right) \tag{14}$$

With:

$$D_{eff} = \frac{k_{eff}}{\rho_f C_f} \tag{15}$$

$$\alpha = \frac{hs_f}{\rho_f C_f} \tag{16}$$

D_{eff} (L^2T^{-1}) is the thermal dispersion and α (T^{-1}) is the exchange coefficient.

The thermal dispersion happens due to hydrodynamic mixing of fluid at the pore scale caused by the nature of the porous medium. Greenkorn (1983) found nine mechanisms responsible of most of the mixing among which the following: 1) Mixing caused by the tortuosity of the flow channels due to obstructions: fluid elements starting a given distance from each other and proceeding at the same velocity will not remain the same distance apart; 2) Existence of autocorrelation in flow paths: in this case, all pores in a porous medium may not be accessible to a fluid element after it has entered a particular flow path; 3) Recirculation due to local regions of reduced pressure due to the conversion of pressure energy into kinetic energy; 4) Hydrodynamic dispersion in a capillary caused by the velocity profile produced by the adhering of the fluid to the wall; 5) Molecular diffusion into dead-end pores: as solute rich front passes the pore. After the front passes, the solute will diffuse back out and thus, dispersing.

Nonlin. Processes Geophys. Discuss., https://doi.org/10.5194/npg-2017-53
Manuscript under review for journal Nonlin. Processes Geophys.
Discussion started: 18 October 2017

263 Using the analogy with the solute transport the Damköhler number Da (Leij et al., 2012) can be
264 introduced in order to evaluate the influence of heat transfer between the fluid and solid phases on
265 the convection phenomena:

266 $$\mathrm{Da} = \frac{\alpha L}{v} \tag{17}$$

267 When Da reaches the unit the heat transfer time scale is comparable with the convection time scale
268 and the LTNE exists between solid and fluid phases. At very high values of Da the heat transfer
269 time scale is much lower than convective time scale and the LTE condition exists between solid and
270 fluid phases. Finally, at very low values of Da the heat transfer phenomena can be neglected.

271 Neglecting the first term on the right side of the Equation 14, the analytical solution of the system
272 equations describing 1D heat transport in semi – infinite domain for instantaneous temperature
273 injection is given by Goltz and Robertz (1986). According to this analytical solution, the probability
274 of density function PDF_{LTNE} of the residence time for LTNE condition can be written as:

275 $$PDF_{LTNE}(x,t) = e^{\alpha t} c_0(x,t) + \alpha \int_0^t H(t,\tau) c_0(x,t)\, d\tau \tag{18}$$

276 With:

277 $$c_0(x,t) = \frac{1}{\sqrt{\pi D_{eff} t}} \exp\left(\frac{x - vt}{4 D_{eff} t}\right) \tag{19}$$

278 $$H(t,\tau) = e^{-\frac{\alpha}{\beta}(t-\tau)-\alpha\tau} \frac{\tau I_1\left(\frac{2\alpha}{\beta}\sqrt{\beta(t-\tau)\tau}\right)}{\sqrt{\beta(t-\tau)\tau}} \tag{20}$$

279 $$\beta = \frac{1-n}{n}\frac{\rho_s c_s}{\rho_f c_f} \tag{21}$$

280 Where I_1 is the modified Bessel function of order 1.

281 The coefficient α can be viewed as the reciprocal of the exchange time required to transfer energy
282 from fluid to solid phase and vice versa. The parameter β (-) represents the ratio between the
283 volume specific heat capacity of the solid phase and the fluid. The effect of local thermal non
284 equilibrium is stronger when the exchange time is the same order of magnitude of the transport
285 time. The local thermal non equilibrium is characterized by thermal distribution profile with a
286 tailing effect.

The observed temperature function $T_{obs}(t)$ at a generic distance x from the injection temperature function $T_{inj}(t)$ can be obtained using the convolution theorem:

$$T_{obs}(x,t) = T_{inj}(0,t) * PDF_{LTNE}(x,t) \quad (22)$$

Experimental setup

The test on convective heat transport in the porous medium has been conducted on a laboratory physical model. Figure 1 shows a sketch of the experimental setup. A plastic circular pipe characterized by a diameter of D = 0.11 m and height of H = 1.66 m has been thermally insulated using a roll of elastomeric foam with a thickness of s = 0.04 m and a thermal conductivity of λ = 0.037 $Wm^{-1}K^{-1}$. The pipe can be filled with different porous materials with different grain sizes and hydrothermal properties. Seven thermocouples have been equally placed along the axis of the pipe with a reciprocal distance of 0.185 m. The first thermocouple is located at a distance of 0.435 m from the inlet of the water. TC08 Thermocouple Data Logger (pico Thecnology) with sampling rate equal to 1 second has been connected with the thermocouples. An adaptable constant head reservoir and an outlet reservoir permit to maintain a constant head during the test and water within the pipe flows from the bottom to the top. An ultrasonic velocimeter (DOP3000 by Signal Processing) is used to measure the instantaneous flow rate. An electric water boiler characterized by a volume equal to 0.01 m^3 has been used to heat the water flowing through the pipe.

A medium gravel (M_1) (USDA, 1975) and a very coarse gravel (M_2) (USDA, 1975) have been used.. The Figure 2 shows the tested materials whereas in Table 1 are reported the hydraulic and the thermal parameters of each material. The grain size and the specific surface of each porous material is directly estimated on a sample of one hundred grains. Whereas the porosity is estimated by the ratio between the volume void space and the total volume of the filled plastic circular pipe. The volume of the void space is obtained measuring the amount of water which enters in the pipe until full saturation. The thermal characteristics reported in the table 1 are literature values (www.engineeringtoolbox.com). The temperature tracer tests involve the observation of the thermal breakthrough curves (BTCs) monitored by the seven thermocouples. Initially cold water flows through the pipe filled with the porous medium in order to have a constant temperature T_0 along the pipe. Subsequently hot water is flows through the pipe, maintaining a constant head condition during the test.

Discussion

317 For each tested porous medium four thermal tracer tests have been carried out varying Re in the
318 range 5.7– 22.5 for M_1 and 23.5 – 105.5 for M_2. The thermal BTCs observed at different distances
319 have been fitted together using equation (19). The root mean square error (RMSE) and the
320 determination coefficient (r^2) have been used as criteria to evaluate the goodness of the fitting. The
321 parameters v, D_{eff} and α have been individually fitted for each thermal tracer test whereas β has
322 been imposed constant for all tracer tests of each tested porous medium. Table 2 shows the
323 estimated values of the heat transport parameters, the RMSE and r^2, whereas figure 3 and figure 4
324 show the fittings results of the observed temperature distribution along the porous column for M_1
325 and M_2 respectively. Table 4 shows the dimensionless numbers Pe, k_{eff}/k_f, Nu and Da evaluated for
326 the different values of Re.

327 As shown in Table 2, the fluid velocity q/n is systematically higher than the estimated thermal
328 convective velocity v for the medium gravel M_1, contrarily for the very coarse gravel M_2 q/n is
329 systematically lower than v.

330 This phenomenon for the coarser material might be attributable to the fact that the heat propagates
331 through both the solid and fluid phase (Anderson, 2005, Rau et al. 2012) and the existence of
332 channeling phenomena that might also have an influence in increasing the convective heat.

333 Even for finer grained materials (2 mm), Rau et al (2012) also found values of thermal velocity
334 systematically lower than solute velocity, coherently with Bodvarssoon (1972), Oldenburg and
335 Pruess (1998), Geiger et al. (2006).

336 Another discrepancy has been observed comparing the values of the porosity presented in table 1
337 and the value of porosity obtained from the equation 18 equal to 0.467 and 0.469 respectively for
338 M_1 and M_2. For M_1 the value of porosity presented in table 1 reaches the value derived from β.
339 Whereas for M_2 the value presented in table 1 is higher than the value derived from β.

340 These results highlight that for M_2 there is the existence of stagnant zones which reduce the amount
341 of porosity that contributes to fluid flow. In other words, in M_1 the total porosity reaches to the
342 effective porosity, whereas in M_2 the effective porosity is less than total porosity.
343 In figure 5 is reported the relationships between Pe and the ratio between the effective thermal
344 conductivity and the fluid thermal conductivity k_{eff}/k_f . The experimental results show a non linear
345 behavior well represented by equation (8). A change of slope is evident changing from M_1 to M_2.
346 The latter material shows a more pronounced thermal dispersion caused by the hydrodynamic
347 mixing of fluid at the pore scale. Some mixing is caused by the tortuosity of the flow paths due to the

presence of obstructions: the fluid elements starting a given distance from each other and proceeding at the same velocity will not remain at the same distance apart. The high level of flow path heterogeneity gives rise to a higher velocity variation at pore scale as well as the presence of the preferential flow paths that enhance the effect of macrodispersion. Mixing can also be caused by recirculation caused by local regions of reduced pressure arising from flow restrictions.

Further mixing can arise from the fact that all pores in a porous medium may not be accessible to a fluid element after it has entered a particular flow path.

These results are coherent with those obtained by Rau et al (2012) who found that the thermal dispersion was transitioning between not depending on the flow velocity and a non linear increase with velocity. They affirmed that the location of the transition zone is a function of the thermal properties of the solid and the sedimentological architecture.

Figure 6 shows the relationship between Pe and Nu. The experimental results highlight that the Nusselt number can be represented by an equation like $Nu = C \times Pe$, where C (-) is a coefficient that assumes a value equal to 0.41 for M_1 and 0.03 for M_2. This coefficient has the physical meaning of the ratio between the surface of the grains in contact with the active flow path that transports heat and the total surface of the grain. M_2 respect to M_1 is characterized by the presence of preferential flow paths and then an equal number of Pe corresponding to a lower Nu because the surface of the grain available to exchange heat between the fluid and solid phase is lower.

As shown in table 3 the Damköhler number Da calculated for M_1 is greater than the unit. Heat exchange is so rapid giving rise to an instantaneous equilibrium between solid and fluid phase. The heat has enough time to diffuse in solid phase. Contrarily Da calculated for M_2 is close to the unit, there is the presence of the local thermal non equilibrium condition.

A comparison of the heat J (ML^2T^{-2}) stored in the porous column per unit temperature difference $\Delta T = T_{inj} - T_0$ (K) varying the specific discharge q for each tested porous medium can be evaluated considering a continuous temperature injection function as:

$$\frac{J}{\Delta T} = \rho_f c_f Q \int_0^{\infty} \left(1 - \int_0^{t} PDF(L,\tau)\, d\tau \right) dt \qquad (23)$$

The combined effects of the flow rate and the particle diameter on heat transfer are illustrated in Figure 7 that shows the variation of the heat stored in the column per unit temperature difference varying the specific discharge for M_1 and M_2. As the flow rate increases, the stored heat increases, and the porous medium with a smaller particle diameter generates a higher increase in heat transfer enhancement than one with a larger particle diameter. This is coherent with the results obtained by Dehghan and Aliparast (2011) and Kifah (2004). M_1 permits to store more heat than M_2. The former

is characterized by a more homogeneous flow path distribution that allows a greater interaction between fluid and solid phase. On the contrary M_2 has a more heterogeneous flow path distribution that increases thermal macrodispersion phenomena at the pore scale and at the same time reduces the interaction between the fluid and solid phase.

In order to put into evidence the performance of the heat transfer enhancement of the porous materials it can be useful to compare the Nusselt number and the hydraulic head loss dh/dx evaluated by equation 1. The Figure 8 shows the ratio between the Nusselt number and head loss as function of the Peclet number. Despite M_1 presents a higher heat transfer enhancement respect to M_2, the head losses are higher and then the ratio between Nu and dh/dx is lower. Furthermore, as Pe increases, the heat transfer enhancement increases more rapidly than the head loss for the fine material M_1, whereas for the coarser material M_2 the opposite happens: increasing the Peclet number the Nusselt number increases weakly due to the presence of channeling phenomena that reduce the heat exchange area between fluid and solid phases.

Conclusion

In this study a laboratory physical model has been set up to analyze the behavior of forced convective heat transport in two porous media characterized by different grain sizes and specific surfaces. For each material four tracer tests have been carried out and they have been compared with the 1D analytical solution of LTNE model. The flow paths heterogeneity that characterizes the coarser material gives rise to a higher velocity variation at pore scale with a channeling effect which causes: 1) the increase in the macrodispersion phenomena in the forced convection heat transport, 2) the decrease in the surface of the grain available to exchange heat between the fluid and solid phase, 3) the presence of the local thermal non equilibrium condition 4) the decrease in the amount of heat that can be stored in the porous medium and 5) a weak growth of heat transfer enhancement respect to the head loss as convective phenomena increases.

The finer material M_1 has a more homogeneous flow path distribution that allows a greater interaction between fluid and solid phase and therefore allows to store more heat than the coarser one.

This can also be seen analyzing the ratio between the Nusselt number and the head loss as function of Peclet number for both materials. Even though the coarser material M_2 is more permeable than M_1 as the advective phenomena increase, the head loss increases more rapidly than the heat transfer

enhancement due to the channeling effect that increases the macrodispersion phenomena and reduces the heat transfer between fluid and solid phase.

The experimental results emphasize the differences between porous and fractured media. As observed by Cherubini at al. (2017) a fractured medium with high density of fractures and then with a higher specific surface is not efficient to store thermal energy because the fractures are surrounded by a matrix with a more limited capacity to store heat. An opposite behavior has been observed in porous media in which a higher specific surface corresponds to a higher capacity to store heat. For porous media as the specific surface decreases the macrodispersion phenomena increase due essentially to the channeling effect and then the surface of the grain available to exchange heat between the fluid and solid phase decreases. Whereas for the fractured media this statement is not true because the macrodispersion phenomena are more related contrarily to the roughness and aperture variation of each single fracture as well as to the connectivity of the fracture network.

The study has increased the understanding of heat transfer processes in the subsurface encouraging the investigation on how further parameters such as the shape and the roughness of the grain of porous media affect the amount of energy that can be stored. This is important to maximize the efficiency and minimize the environmental impact of the geothermal installations in groundwater.

References

Ait Saada, M., Chikh, S. and Campo, A. (2006). Analysis of hydrodynamic and thermal dispersion in porous media by means of a local approach. Heat and Mass Transfer September 2006, Volume 42, Issue 11, pp 995–1006

Amiri, A. and Vafai, K. (1994). Analysis of Dispersion Effects and Nonthermal Equilibrium, Non-Darcian, Variable Porosity, Incompressible Flow Through Porous Media, Int. J. Heat Mass Transf., 37, pp. 939–954.

Anderson, M. P. (2005), Heat as a ground water tracer, Ground Water, 43(6), 951–968, doi:10.1111/j.1745-6584.2005.00052.x.

Bodvarsson, G. (1972), Thermal problems in the siting of reinjection wells, Geothermics, 1(2), 63–66, doi:10.1016/0375-6505(72)90013-2

Dehghan, H. and Aliparast, P. (2011) An Investigation into the Effect of Porous Medium on Performance of Heat Exchanger World Journal of Mechanics, 2011, 1, 78-82 doi:10.4236/wjm.2011.13011 Published Online June 2011

Amiri, A., and Vafai, K. (1998). Transient Analysis of Incompressible Flow Through a Packed Bed, Int. J. Heat Mass Transf., 41, pp. 4259–4279.

443 Anderson, M. P. (2005), Heat as a ground water tracer, Ground Water, 43(6), 951–968,
444 doi:10.1111/j.1745-6584.2005.00052.x
445 Eidsath A, Carbonell RG, Whitaker S, Herrmann LR (1983) Dispersion in pulsed systems. Part III,
446 comparison between theory and experiments in packed beds. Chem Eng Sci 38:1803–1816
447 Emmanuel, S and Berkowitz B. (2007). Continuous time random walks and heat transfer in porous
448 media Transp Porous Med (2007) 67:413–430
449 Geiger, S., T. Driesner, C. A. Heinrich, and S. K. Matthai (2006), Multiphase thermohaline
450 convection in the earth's crust: I. A new finite element-finite volume solution technique combined
451 with a new equation of state for NaCl-H2O, Transp. Porous Media, 63(3), 399–434, doi:10.
452 1007/s11242-005-0108-z.
453 Goltz, M. N. and Roberts, P. V. (1986). Three-dimensional solutions for solute transport in an
454 infinite medium with mobile and immobile zones, Water Resour. Res., 22, 1139–1148, 1986
455 Greenkorn R.A. (1983). Flow phenomena in porous media, Marcel Dekker, INC., New York and Besel,
456 1983.
457 Gunn. D.G. and Pryce, C. (1969) Dispersion in packed beds. Trans Inst Chem Eng 47:341–350
458 Hadim, A. (1994). Forced Convection in a Porous Channel With Localized Heat Sources, ASME J.
459 Heat Transfer, 116, pp. 465–472.
460 Hsu, C. T., and Cheng P. (1990), Thermal dispersion in a porous medium, Int. J. Heat Mass
461 Transfer, 33(8), 1587–1597, doi:10.1016/0017-9310(90)90015-m
462 Hwang, G. J., Wu, C. C., and Chao, C. H. (1995). Investigation of Non-Darcian Forced Convection
463 in an Asymmetrically Heated Sintered Porous Channel, ASME J. Heat Transfer, 117, pp. 725–732.
464 Ingebritsen, S.E., Stanford, W.E. (1999). Groundwater in geologic processes. Cambridge University
465 Press, 1999.
466 Khalil R. A., El-Shazly, K.M. and Assasa G. R. (2000). Heat transfer and fluid flow characteristics
467 of forced convection through a packed pipe 11th International mechanical Power Engineering
468 Conference (IMPECll),Cairo, Feb (5-7), 2000
469 Kamiuto K and Saitoh S. (1994), Fully Developed Forced-Convection Heat Transfer in Cylindrical
470 Packed Beds With Constant Wall Temperatures, JSME International Journal, Series B. Vol. 37,
471 No.3, pp. 554-559.
472 Kaviany, M. (1985). Laminar flow through a porous channel bounded by isothermal parallel plates,
473 Int. J. Heat Mass Transf., 28, pp. 851–858.
474 Kaviany, M. (1995). Principles of Heat Transfer in Porous Media, 2nd Edition, New York,
475 Springer-Verlag, 1995.

476 Kifah 2004. Fluid flow and heat transfer Characteristics in a Vertical Tube Packed Media, Ph.D
477 Thesis University of Technology.
478 Koch, D.L., Cox, R.G., Brenner, H. and Brady, J.F. (1989) The effect of order on dispersion in
479 porous media. J Fluid Mech 200:173–188
480 Koh, J. C. Y. and Colony R. (1974). Analysis of cooling effectiveness for porous material in a
481 coolant passage, J.Heat Transfer 96, 324-330 (1974).
482 Koh, J.C.Y. and Stevens, R.L. (1975). Enhancement of Cooling Effectiveness for Porous Material
483 in Coolant Passages. ASME Journal of Heat Transfer, Vol.96, pp. 324-330.
484 Kuwahara, F., Shirota, M. and Nakayama, A.. (2001). A numerical study of interfacial convective
485 heat transfer coefficient in two-equation model for convection in porous media, International
486 Journal of Heat and Mass Transfer 44 (2001) 1153–1159.
487 Lauriat, G., and Vafai, K. (1991). Forced Convective Flow and Heat Transfer Through a Porous
488 Medium Exposed to a Flat Plate or a Channel, Convective Heat and Mass Transfer in Porous
489 Media, S. Kacac, B. Kilikis, F. A. Kulacki, and F. Arnic, eds., Kluwer Academic, Dordrecht, pp.
490 289–328.
491 Leij F. J., Toride N., Field M. S. and Scortino S. (2012). Solute transport in dual-permeability
492 porous media. Water Resource Research VOL. 48, W04523, doi:10.1029/2011WR011502, 2012.
493 Lu, X., Ren, T. and Gong, Y. (2009). Experimental investigation of thermal dispersion in saturated
494 soils with one-dimensional water flow. Soil Science Society of America Journal, 73(6), 2009:
495 1912-1920.
496 Metzger, T., Didierjean, S. and Maillet, D. (2004). Optimal experimental estimation of thermal
497 dispersion coefficients in porous media., International Journal of Heat and Mass Transfer, 47(14),
498 2004: 3341-3353.
499 Minkowycz, W.J., Haji-Sheikh, A. and Vafai K. (1999) On departure from local thermal
500 equilibrium in porous media due to a rapidly changing heat source: the Sparrow number
501 International Journal of Heat and Mass Transfer, 42, 3373-3385.
502 Molina-Giraldo, N., Bayer, P. and Blum, P. (2011). Evaluating the influence of thermal dispersion
503 on temperature plumes from geothermal systems using analytical solutions. International Journal of
504 Thermal Sciences, 50(7), 2011: 1223-1231.
505 Mori, Y., Hopmans, J.W., Mortensen, A.P. and Kluitenberg, G.J. (2005). Estimation of vadose zone
506 water flux from multifunctional heat pulse probe measurements. Soil Science Society of America
507 Journal, 69(3), 2005: 599- 606.
508 Nield, D.A. and Bejan, A. (2006). Convection in porous media. Springer, 2006

509 Oldenburg, C. M., and K. Pruess (1998), Layered thermohaline convection in hypersaline
510 geothermal systems, Transp. Porous Med, 33(1–2), 29–63, doi:10.1023/a:1006579723284.
511 Özgümüş, T., Mobedi, M. Özkol Ü. and Nakayama A. (2011) Thermal Dispersion in Porous Media
512 –A Review on Approaches in Experimental Studies 6th International Advanced Technologies
513 Symposium (IATS'11), 16-18 May 2011, Elazığ, Turkey
514 Rau, G.C., Andersen, M.S. and Acworth, R. I. (2012). Experimental investigation of the thermal
515 dispersivity term and its significance in the heat transport equation for flow in sediments., Water
516 Resources Research, 48(3) 2012.
517 Sauty, J., Gringarten, A., Menjoz, A., and Landel, P. (1982). Sensible energy storage in aquifers: 1.
518 Theoretical study, 18(1), 1982: 245-252.
519 Smith, L. and Chapman, D.S. (1983). On the thermal effects of groundwater flow: 1. Regional scale
520 systems., Journal of Geophysical Research, 88(B1), 1983: 593-608.
521 Soil Survey Staff, 1975. Soil taxonomy: a basic system of soil classification for making and
522 interpreting soil surveys, USDArSCS Agricultural Handbook No. 436. U.S. Government Printing
523 Office, Washington, DC
524 Vafai, K. and Tien C. I. (1981). Boundary and Inertia effects on flow and heat transfer in porous
525 media, Int. J. Heat Transfer 24, 195-203 .
526 Vafai, K. and Tien C. I. (1982). Boundary and inertia effects on convective mass transfer in porous
527 media, Int. J. Heat Transfer 25, 1183-1190
528 Vandenbohede, A., Louwyck, A. and Lebbe, L. (2009). Conservative solute versus heat transport in
529 porous media during push-pull tests. Transport in porous media, 76(2), 2009: 265-287.
530 Vafai, K., and Kim, S. J., (1989). Forced Convection in a Channel Filled With a Porous Medium:
531 An Exact Solution, ASME J. Heat Transfer, 111, pp. 1103–1106.
532 Wu, C.C. and Hwang, G.J. (1998). Flow and heat transfer characteristics inside packed and
533 fluidized beds. J. Heat Trans.120 , 667–673 (1998)
534

Nonlin. Processes Geophys. Discuss., https://doi.org/10.5194/npg-2017-53
Manuscript under review for journal Nonlin. Processes Geophys.
Discussion started: 18 October 2017

Nonlinear Processes in Geophysics
Discussions
Open Access
EGU

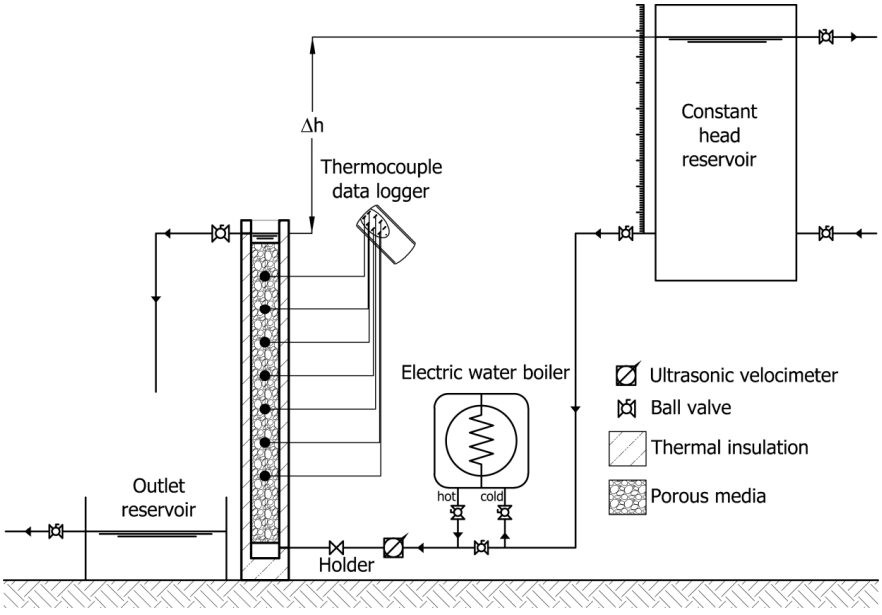

535

536 **Figure 1. Setup of experimental apparatus**

537

538 **Figure 2. Samples of the materials used for the experiments with different average grain sizes d_p. a) d_p = 9.2 mm b) d_p = 41.6**
539 **mm.**

	M_1	M_2
Porosity (-)	0.47	0.53
Average grain size (mm)	9.21	41.65
Average specific surface (m^{-1})	675.80	148.4
Soild density ($Kg \cdot m^{-3}$)	2210	2210
Soil heat capacity ($J \cdot Kg^{-1} \cdot K^{-1}$)	840	840
Soil thermal conductivity ($W \cdot m^{-1} \cdot K^{-1}$)	2.15	2.15

540 **Table 1. Properties of the porous materials**

Re	$q/n \times 10^{-2}$ (m/s)	$v \times 10^{-2}$ (m/s)	$D_{eff} \times 10^{-3}$ (m^2/s)	α (s^{-1})	β (-)	RMSE	r^2

Nonlin. Processes Geophys. Discuss., https://doi.org/10.5194/npg-2017-53
Manuscript under review for journal Nonlin. Processes Geophys.
Discussion started: 18 October 2017

M_1	5.7	0.134	0.109	0.099	0.144		75.659	0.9781
	9.5	0.223	0.222	0.102	0.260		4.835	0.9958
	15.5	0.361	0.321	0.116	0.403		1.176	0.9984
	22.5	0.525	0.486	0.126	0.767	0.480	0.033	0.9999
M_2	23.5	0.106	0.138	0.165	0.003		29.740	0.9815
	46.9	0.211	0.248	0.273	0.006		7.843	0.9886
	69.3	0.312	0.367	0.409	0.008		4.742	0.9904
	105.5	0.475	0.579	0.655	0.012	0.476	1.747	0.9944

Table 2. Estimated values of parameters for LTNE model for different Re values.

	Re	Pe	k_{eff}/k_f	Nu	Da
M_1	5.7	70.05	688.83	26.51	146.28
	9.5	142.49	711.48	47.98	130.18
	15.5	205.95	811.60	74.30	139.47
	22.5	311.64	882.13	141.45	175.46
M_2	23.5	402.32	1148.61	11.32	2.10
	46.9	721.64	1902.80	25.21	2.61
	69.3	1068.78	2856.49	33.52	2.34
	105.5	1684.17	4568.91	50.84	2.25

Table 3. Dimensionless numbers Pe, k_{eff}/k_f, Nu and Da calculated for different Re values.

Nonlin. Processes Geophys. Discuss., https://doi.org/10.5194/npg-2017-53
Manuscript under review for journal Nonlin. Processes Geophys.
Discussion started: 18 October 2017

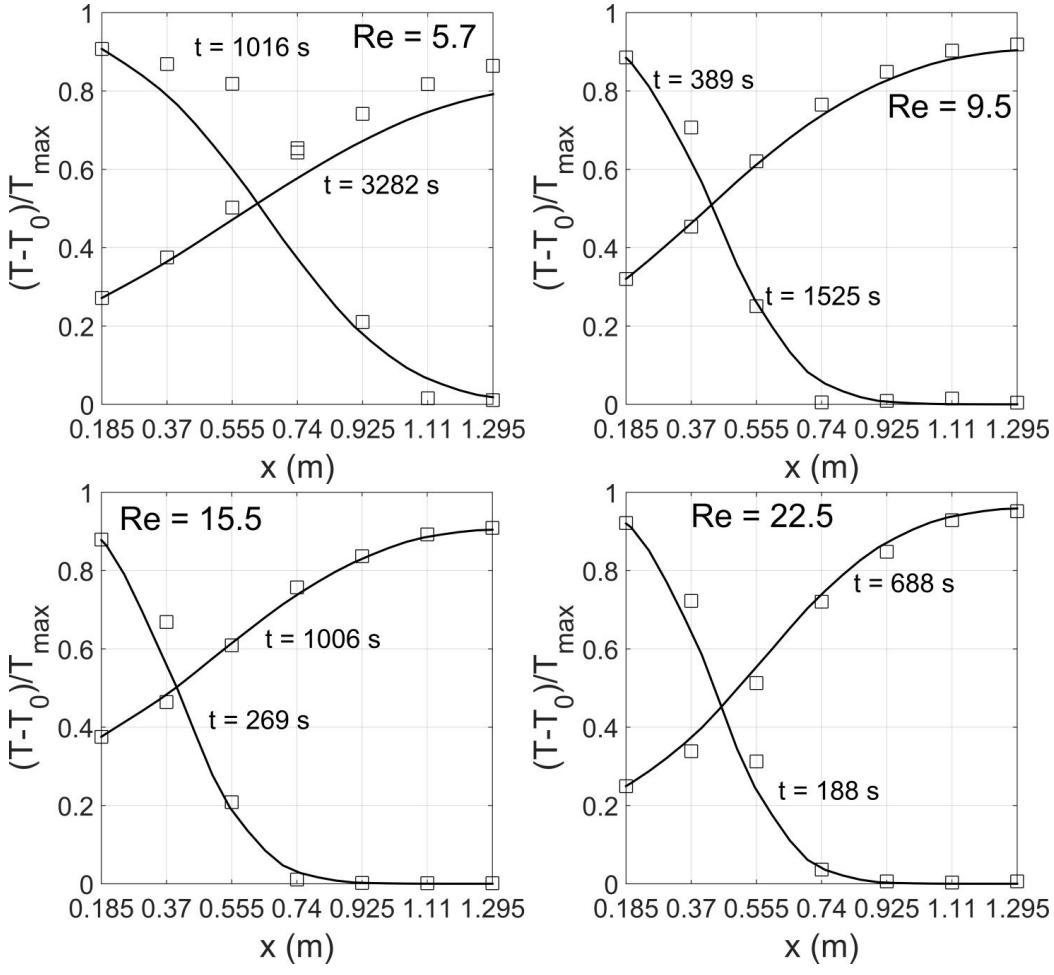

543

544 **Figure 3. Temperature distribution for different Re values along the porous column filled with material M_1. Squares**
545 **represent the experimental values, the continuous lines represent the simulated values.**

Nonlin. Processes Geophys. Discuss., https://doi.org/10.5194/npg-2017-53
Manuscript under review for journal Nonlin. Processes Geophys.
Discussion started: 18 October 2017

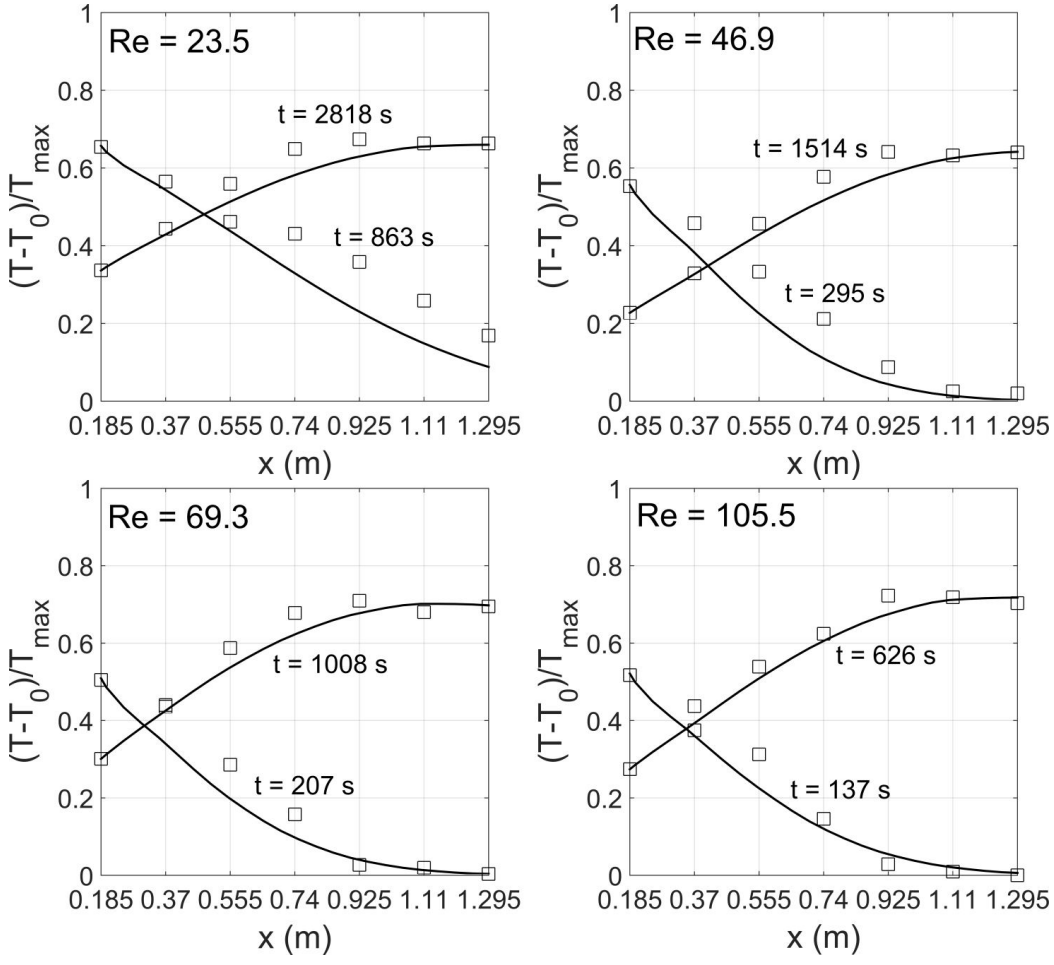

546

547 **Figure 4. Temperature distribution for different Re values along the porous column filled with material M_2. Squares**
548 **represent the experimental values, continuous lines represent the simulated values.**

Nonlin. Processes Geophys. Discuss., https://doi.org/10.5194/npg-2017-53
Manuscript under review for journal Nonlin. Processes Geophys.
Discussion started: 18 October 2017

Nonlinear Processes in Geophysics
Discussions
Open Access
EGU

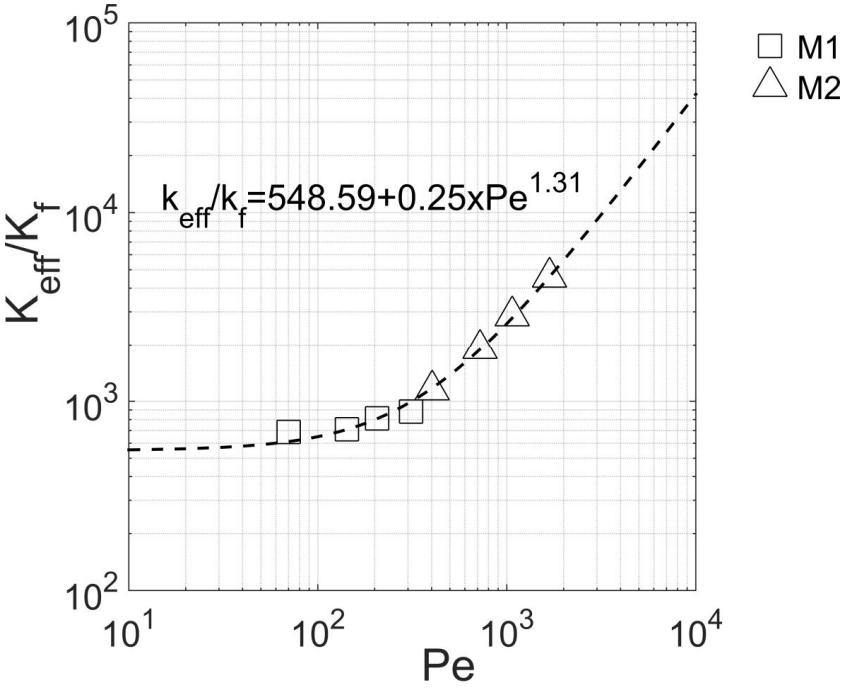

549

550 **Figure 5. Relationship between *Pe* and k_{eff}/k_f.**

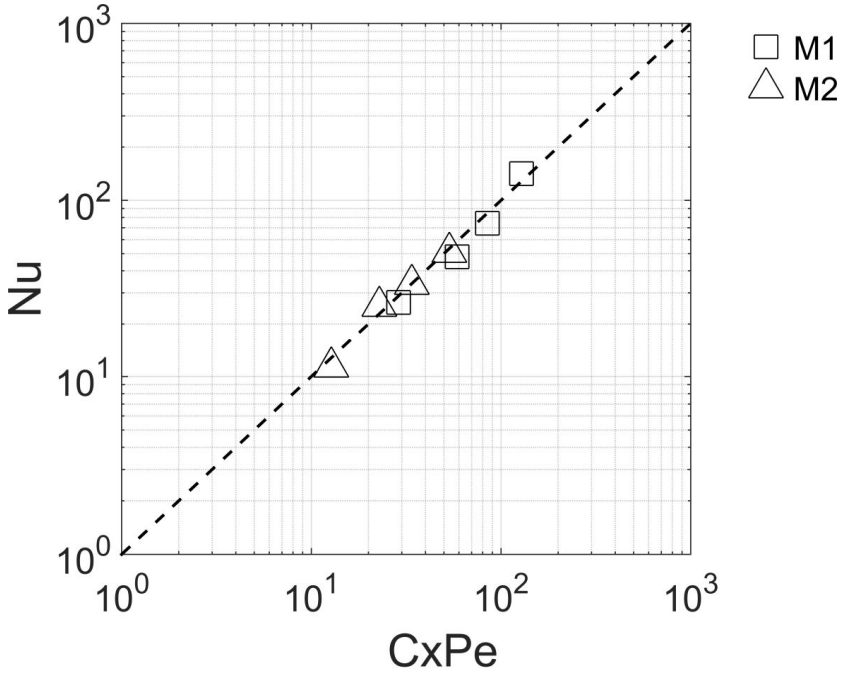

551

552 **Figure 6. Relationship between C×Pe and Nu.**

Nonlin. Processes Geophys. Discuss., https://doi.org/10.5194/npg-2017-53
Manuscript under review for journal Nonlin. Processes Geophys.
Discussion started: 18 October 2017

Nonlinear Processes in Geophysics
Discussions
Open Access
EGU

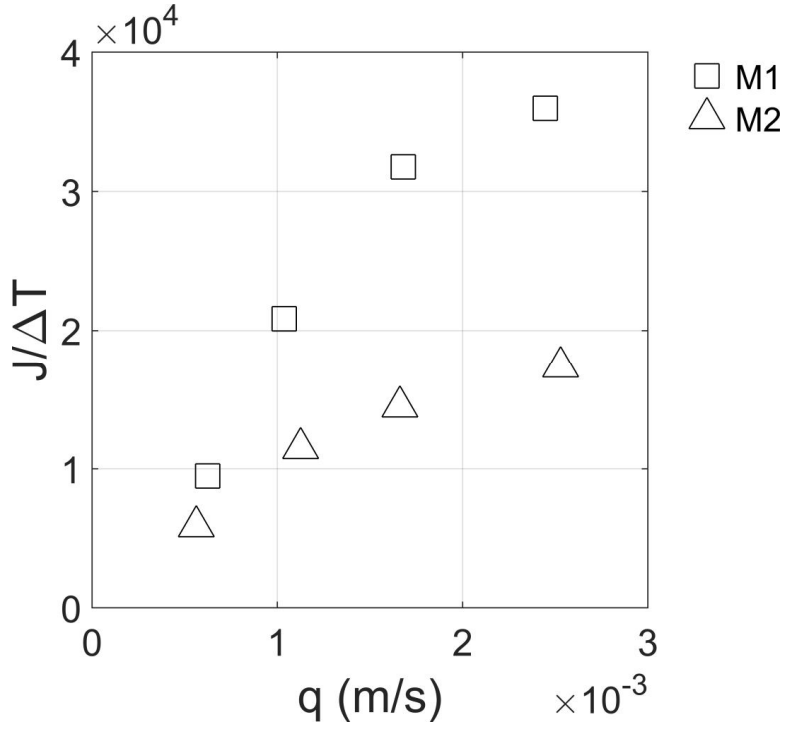

553

554 **Figure 7. heat exchanged $J/(T_{inj} - T_0)$ varying the specific rate q (m/s).**

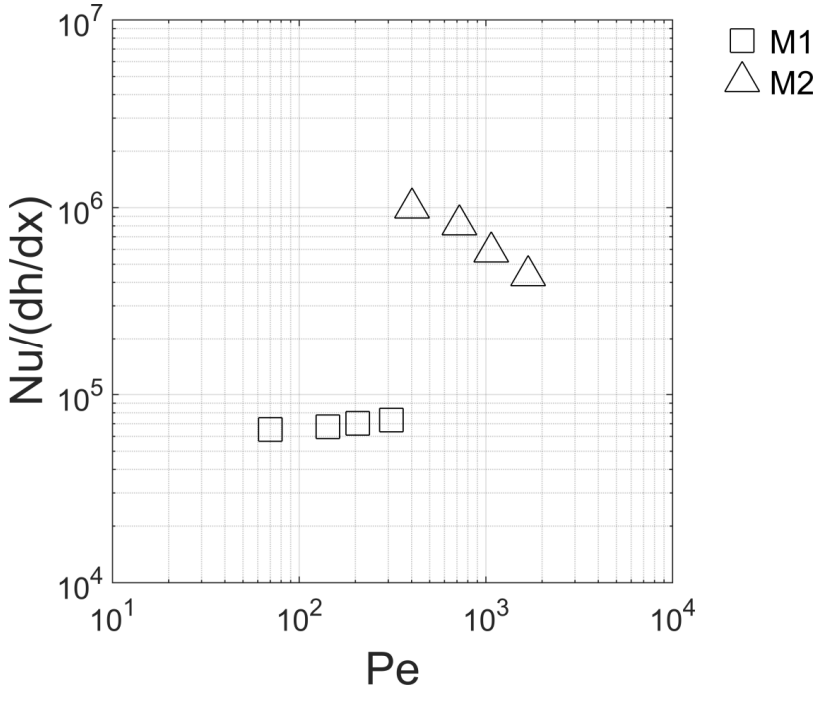

555

Nonlin. Processes Geophys. Discuss., https://doi.org/10.5194/npg-2017-53
Manuscript under review for journal Nonlin. Processes Geophys.
Discussion started: 18 October 2017

556

557 **Figure 8. Nusselt number – head loss ratio varying Peclet number.**